Acta Mechanica 187, 37–53 (2006)
DOI 10.1007/s00707-006-0335-6

Acta Mechanica
Printed in Austria

Flow of pressure-dependent plastic material between two rough conical walls

S. Alexandrov and **E. Lyamina**, Moscow, Russia

Received January 11, 2006
Published online: April 20, 2006

Summary. The objectives of the present paper are to find solutions for axisymmetric flow of pressure-dependent material between two rough conical walls and to compare the qualitative behavior of the solutions based on two models of pressure-dependent plasticity, the coaxial model and the double-shearing model. The constitutive equations of each model reduce to classical plasticity of pressure-independent material at specific values of the input parameters. Nevertheless, the solution behavior essentially depends on the model chosen, independently of how close the input parameters are to these specific values. In particular, such features of the solutions as the friction regime and singularity are emphasized. It is concluded that the double-shearing model only retains all features inherent to classical plasticity.

1 Introduction

Flow of plastic material through an infinite conical channel is one of the classical problems of plasticity theory. For rigid perfectly plastic material obeying different pressure-independent yield criteria the solutions to this problem have been proposed in [1]–[4]. The main assumption accepted in these works is that the radial velocity in a spherical coordinate system is the only non-zero velocity component. Attempts to extend this assumption to other material models have been made in [5]–[8]. However, it is possible to verify by inspection that the solutions [5], [6] for viscoplastic materials and the solution [7] for linear/hardening materials do not exist in the case of the maximum friction law. For such material models this law postulates that the friction stress is equal to the local shear yield stress. On the other hand, the solution based on the double-shearing model (both the model and solution are described in [8]) retains all qualitative properties of the solutions given in [1]–[4]. For this material model the maximum friction law requires that the friction surface coincides with an envelope of characteristics. However, many theories of pressure-dependent plasticity have been proposed (reviews can be found, for example, in [8] and [9]) but none of them has found general acceptance. Moreover, though most of these theories reduce to classical plasticity at specific values of input parameters, the solution behavior essentially depends on the model chosen, independently of how close the input parameters are to these specific values [10]–[12]. It seems that comparison of the qualitative behavior of solutions based on different models can help to choose an appropriate model for specific applications. For instance, some metal alloys reveal pressure-dependence of the yield condition [13], [14]. For such materials, it is natural to require that main features

inherent to solutions of classical plasticity are retained in the corresponding solutions based on a pressure-dependent theory of plasticity. In [10]–[12], several plane-strain closed-form solutions have been compared and in [11] and [12] the difference in solution behavior has been explained by the structure of characteristic curves. Therefore, it is of interest to compare solutions based on models whose equations are not hyperbolic. In the present paper the axisymmetric flow between two rough conical surfaces where the maximum friction law is assumed is considered. Solutions based on the double-shearing and coaxial models are proposed and analyzed.

In the case of the double-shearing model the solution is singular, as also follows from the general theory [15]. The same singular behavior of solutions occurs in the classical plasticity of rigid perfectly plastic solids [16]. Using this feature of solutions the strain rate intensity factor has been introduced in [16] for rigid perfectly plastic materials and in [17] for materials obeying the double-shearing model. The concept of the strain rate intensity factor can be used to describe physical processes in a narrow layer near frictional interfaces and to predict the thickness of the layer of intensive deformation in the vicinity of frictional interfaces [18], [19]. An advantage of the problem under consideration is that there are two maximum friction surfaces. Therefore, it is possible to reveal a qualitative effect of the strain rate intensity factor on physical processes in the vicinity of the friction surfaces, according to the theories [18], [19], without having numerical values of parameters involved in the theories. In general, this effect can be observed experimentally.

2 Statement of the problem

The geometry of the process and the spherical coordinate system $\rho\theta\varphi$ are shown in Fig. 1. The material flows between two rough conical surfaces whose equations are $\theta = \theta_0$ and $\theta = \theta_1$.

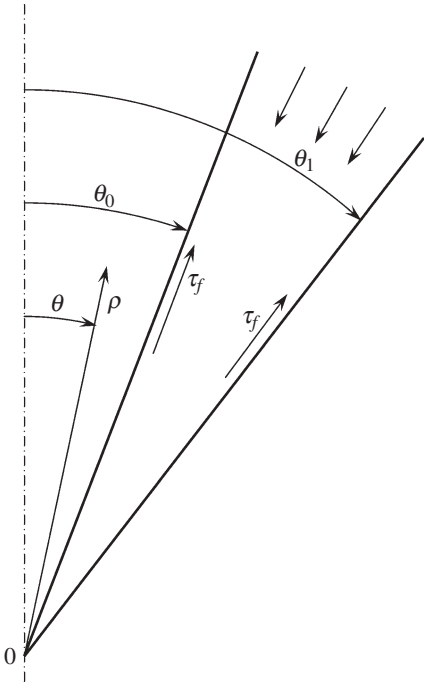

Fig. 1. Notation for flow between two conical walls

Because of axial symmetry, the solution is independent of φ. The friction stresses, τ_f, are directed as shown in Fig. 1. It is supposed that the friction stress attains its maximum possible magnitude admissible by the material model (maximum friction law). Note that in the case of pressure-independent plasticity this magnitude can be directly found from the yield criterion and is simply the local shear yield stress, independently of the state of stress at the point of interest. However, yield criteria of pressure-dependent plasticity permit infinite shear stresses and, therefore, the aforementioned definition for the maximum friction law is not valid. On the other hand, solutions to particular problems show that there is a maximum possible shear stress at the friction surface (no solution exists for a higher friction stress) [10]–[12], [20]–[24]. In all of these cases, however, a system of hyperbolic equations has been solved and the maximum friction law has been introduced by the condition that the friction surface coincides with an envelope of characteristics. In the present paper, the equations of one of the models adopted are not hyperbolic. Therefore, the maximum friction law will be formulated separately for each of the models considered. There are no other stress boundary conditions.

Let u_ρ, u_θ and u_φ be the velocity components in the spherical coordinate system. The velocity boundary conditions are $u_\theta = 0$ at $\theta = \theta_0$ and $\theta = \theta_1$. A typical assumption to find a solution for flow through infinite channels is $u_\theta = 0$ and $u_\varphi = 0$ everywhere, for example [1], [2]. Therefore, the velocity boundary conditions are automatically satisfied. Moreover, the solution to the incompressibility equation is

$$u_\rho = -\frac{Q}{\rho^2} h(\theta), \tag{1}$$

where Q is the volume flux and $h(\theta) > 0$ is an arbitrary function of θ.

3 Double-shearing model

A complete description of the model is given in [8]. Let $\sigma_{\rho\rho}$, $\sigma_{\theta\theta}$, $\sigma_{\varphi\varphi}$, and $\sigma_{\rho\theta}$ be the stress components in the spherical coordinate system. In the case under consideration $\sigma_{\varphi\varphi}$ is also one of the principal stresses, and the state of stress should correspond to the edge of Coulomb-Mohr yield surface defined by the following equations [8]

$$\sigma_1(1 + \sin\phi) = 2c\cos\phi + \sigma_{\varphi\varphi}(1 - \sin\phi), \quad \sigma_2 = \sigma_{\varphi\varphi}, \tag{2.1,2}$$

where σ_1 and σ_2 are the principal stresses in the $\rho\theta$ planes, ϕ is the angle of internal friction and c is the cohesion. Using the standard substitution [8]

$$\sigma_{\rho\rho} = -p + q\cos 2\psi, \quad \sigma_{\theta\theta} = -p - q\cos 2\psi, \quad \sigma_{\varphi\varphi} = -p - q, \quad \sigma_{\rho\theta} = q\sin 2\psi, \tag{3.1–4}$$

it is possible to show that Eq. (2.2) is automatically satisfied and Eq. (2.1) reduces to

$$p\sin\phi = q - c\cos\phi. \tag{4}$$

In (3) and what follows, ψ is the angle the σ_1 principal stress direction makes with the direction of ρ and $q \geq 0$. Equations (3) and (4) should be complemented with the equilibrium equations in the form

$$\begin{aligned} &\rho\frac{\partial\sigma_{\rho\rho}}{\partial\rho} + \frac{\partial\sigma_{\rho\theta}}{\partial\theta} + 2\sigma_{\rho\rho} - \sigma_{\theta\theta} - \sigma_{\varphi\varphi} + \sigma_{\sigma\theta}\cot\theta = 0, \\ &\rho\frac{\partial\sigma_{\rho\theta}}{\partial\rho} + \frac{\partial\sigma_{\theta\theta}}{\partial\theta} + \left(\sigma_{\theta\theta} - \sigma_{\varphi\varphi}\right)\cot\theta + 3\sigma_{\rho\theta} = 0. \end{aligned} \tag{5}$$

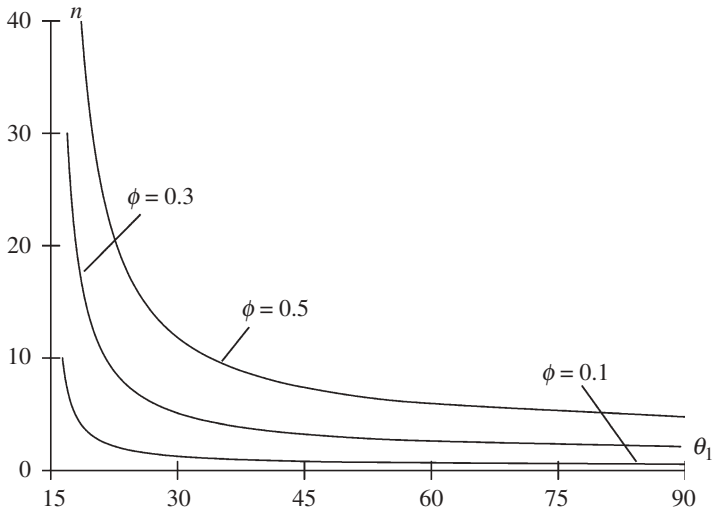

Fig. 2. Variation of n-value with the angle θ_1 at different values of ϕ and $\theta_0 = 15^0$

A typical assumption to find a solution for flow through infinite channels is that ψ is independent of ρ, for example [1], [2]. Equations (3) through (5) are compatible with this assumption if

$$q = \exp[f(\theta)]\rho^n, \tag{6}$$

where f is an arbitrary function of θ and n is an arbitrary constant. Then, Eqs. (5), with the use of (3) and (4), transform to

$$\frac{d\psi}{d\theta} = \frac{n\cos^2\phi - \sin\phi[3\sin\phi + 1 + \cos 2\psi(3 + \sin\phi) + \cot\theta\sin 2\psi(1 + \sin\phi)]}{2\sin\phi(\sin\phi + \cos 2\psi)}, \tag{7}$$

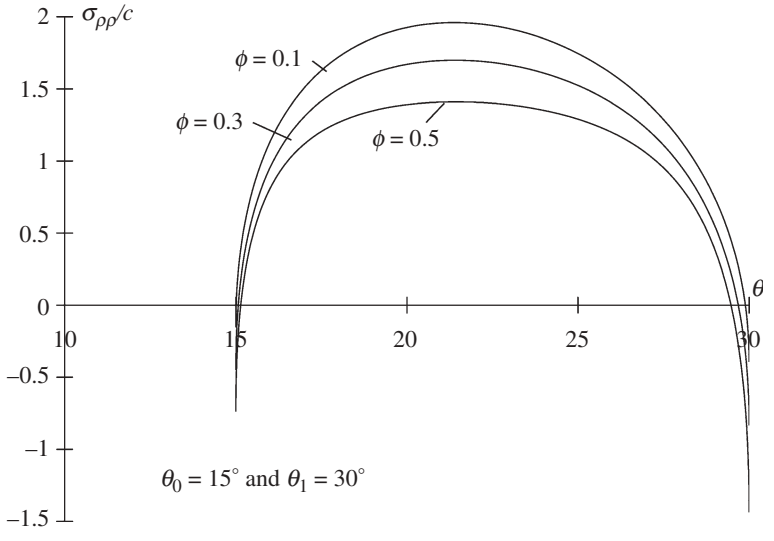

Fig. 3. Variation of the dimensionless stress $\sigma_{\rho\rho}/c$ with the angle θ at $\rho = 1$

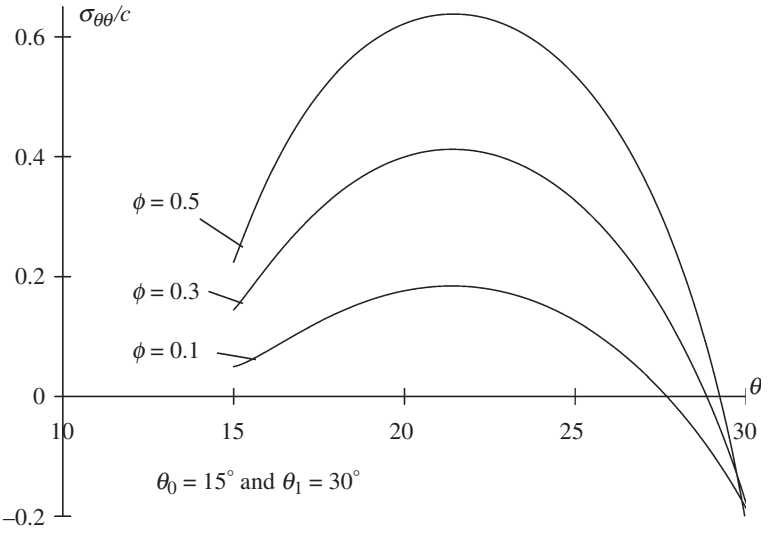

Fig. 4. Variation of the dimensionless stress $\sigma_{\theta\theta}/c$ with the angle θ at $\rho = 1$

$$\frac{df}{d\theta} = \frac{n \sin 2\psi - \sin\phi[\cot\theta(1 - \cos 2\psi) + \sin 2\psi]}{\sin\phi + \cos 2\psi}. \tag{8}$$

These equations should be solved numerically. It is known that the system of equations consisting of (3) through (5) is hyperbolic and its characteristics are inclined to the ρ-direction at $\psi \pm (\pi/4 + \phi/2)$ [8]. Since an envelope of characteristics is a natural boundary of analytic solutions, the maximum friction law can be formulated as the condition that the friction surface coincides with an envelope of characteristics. Such a formulation of the friction law has already been used in plane strain and axisymmetric problems for materials obeying the double-shearing model [10]–[12], [20]–[24]. Moreover, in the case of rigid perfectly plastic materials, this formulation is equivalent to the conventional formulation of the maximum friction law that the

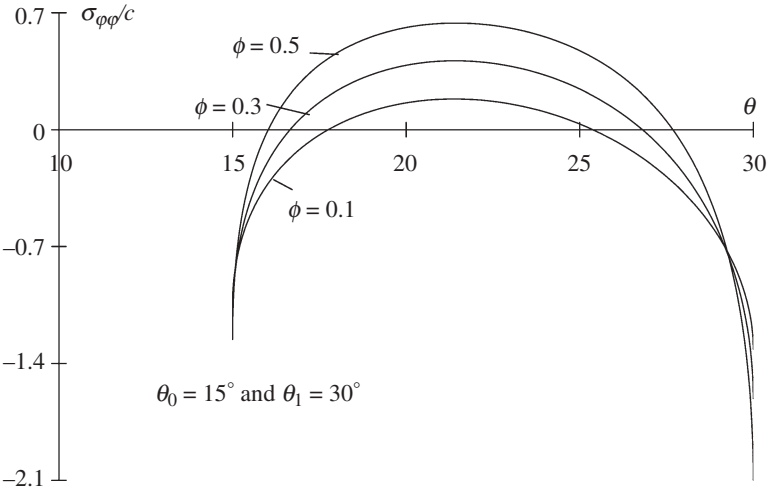

Fig. 5. Variation of the dimensionless stress $\sigma_{\varphi\varphi}/c$ with the angle θ at $\rho = 1$

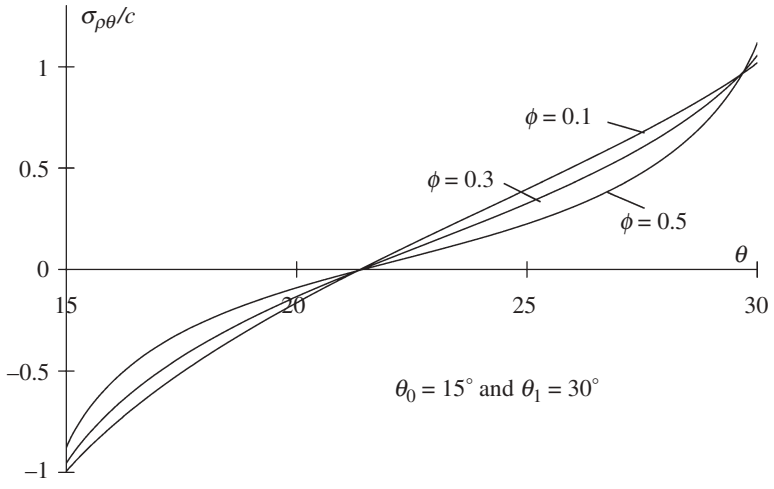

Fig. 6. Variation of the dimensionless stress $\sigma_{\rho\theta}/c$ with the angle θ at $\rho = 1$

friction stress is equal to the maximum shear yield stress. Therefore, taking into account the direction of the friction stresses (Fig. 1) and Eq. (3.4) it is possible to get the following conditions on ψ:

$$\psi = -\left(\frac{\pi}{4} + \frac{\phi}{2}\right) \tag{9}$$

at $\theta = \theta_0$ and

$$\psi = \frac{\pi}{4} + \frac{\phi}{2} \tag{10}$$

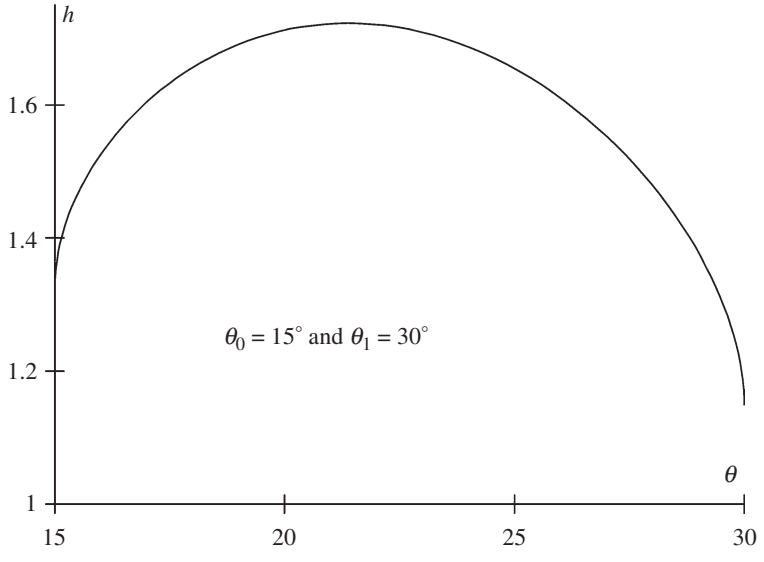

Fig. 7. Variation of h with the angle θ at $\phi = 0.1$

at $\theta = \theta_1$. Solving Eq. (7), with the use of the conditions (9) and (10), it is possible to find n and the distribution of ψ. It is seen from the structure of Eq. (7) that $|d\psi/d\theta| \to \infty$ as $\theta \to \theta_0$ and $\theta \to \theta_1$. Therefore, it is more convenient to solve (7) for θ as a function of ψ. Figure 2 illustrates the dependence of n on parameters of the process and material. It is seen from this figure that $n > 0$. Therefore, as follows from Eq. (6), $q \to 0$ as $\rho \to 0$. Then, Eqs. (3) show that $\sigma_{\rho\rho} = \sigma_{\theta\theta} = \sigma_{\varphi\varphi} = -p$ at $\rho = 0$. Thus the state of stress at this point corresponds to the vertex of the yield surface. In order to find the stress distribution, it is necessary to solve Eq. (8). It is seen from the structure of this equation that $|df/d\theta| \to \infty$ as $\theta \to \theta_0$ and $\theta \to \theta_1$. To exclude this singularity, it is possible to represent the left hand side of (8) in the form $(df/d\psi)(d\psi/d\theta)$ and, then, to replace $d\psi/d\theta$ with the right hand side of (7). It is also necessary to replace θ with a function of ψ by means of the solution to Eq. (7). The resulting equation can be solved numerically with no difficulty. However, there is no natural boundary condition for this equation. It is typical for this kind of problems, for example [1]–[4]. Therefore, to illustrate the dependence of stress components of the angle θ, Eq. (8) has been solved with the condition $f = 0$ at $\theta = \theta_0$ and, then, Eqs. (3) and (4) have been used. The variation of dimensionless stress components with θ is shown in Figs. 3–6 at $\rho = 1$. The parameters of the process and material used are shown in the figures.

The velocity equations of the double-shearing model are given in [8]. In the case under consideration, those are reduced to the incompressibility equation and the following equation:

$$2\xi_{\rho\theta}\cos 2\psi - \left(\xi_{\rho\rho} - \xi_{\theta\theta}\right)\sin 2\psi + 2\sin\phi\left(\omega_{\rho\theta} + d\psi/dt\right) = 0, \tag{11}$$

where $\xi_{\rho\rho}$, $\xi_{\theta\theta}$ and $\xi_{\rho\theta}$ are the strain rate components in the spherical coordinate system, $\omega_{\rho\theta}$ is the component of spin in the same system, and $d\psi/dt$ is the time derivative of ψ. The incompressibility equation is satisfied due to (1). Since the flow is steady, $u_\theta = 0$, $u_\varphi = 0$ and $\partial\psi/\partial\rho = 0$, the derivative $d\psi/dt$ vanishes everywhere. Then, Eq. (11) can be rewritten, with the use of (1), in the form

$$\frac{dh}{d\theta} = -\frac{3h\sin 2\psi}{(\sin\phi + \cos 2\psi)}. \tag{12}$$

Using Eq. (7), this equation can be transformed to

$$\frac{dh}{d\psi} = -\frac{6\sin\phi h\sin 2\psi}{n\cos^2\phi - \sin\phi[3\sin\phi + 1 + \cos 2\psi(3 + \sin\phi) + \cot\theta\sin 2\psi(1 + \sin\phi)]}. \tag{13}$$

The solution to (7) should be used to exclude θ on the right hand side of this equation. Since the volume flux is defined by

$$Q = 2\pi\rho^2 \int_{\theta_0}^{\theta_1} u_\rho \sin\ \theta d\theta, \tag{14}$$

the substitution of Eq. (1) into (14) gives

$$1 = 2\pi \int_{\theta_0}^{\theta_1} h(\theta)\sin\theta\ d\theta. \tag{15}$$

Using Eq. (7), this equation can be rewritten in the form

$$\frac{1}{4\pi\sin\phi} = \int_{-\pi/4-\phi/2}^{\pi/4+\phi/2} \frac{h(\psi)(\sin\phi+\cos 2\psi)\sin\theta}{n\cos^2\phi-\sin\phi[3\sin\phi+1+\cos 2\psi(3+\sin\phi)+\cot\theta\sin 2\psi(1+\sin\phi)]}d\psi. \tag{16}$$

The solution to (7) should be used to exclude θ in the integrand on the right hand side of (16). The solution to Eq. (13) should satisfy (16). The numerical solution for h is illustrated in Fig. 7. The difference between the curves for $\phi = 0.1$, $\phi = 0.3$ and $\phi = 0.5$ is very small. Therefore, the single curve in Fig. 7 corresponding to $\phi = 0.1$ represents, in fact, all three cases.

4 Coaxial model

The original model has been proposed for plane strain deformation. In this case the only difference from the double-shearing model is that the coaxial model including the condition of coaxiality of the stress and stain rate tensors instead of an equation similar to (11). To extend the coaxial model to three-dimensional deformation, it is necessary to choose a corresponding yield criterion. An appropriate yield criterion is

$$\alpha\sigma + \sigma_{eq} = \sigma_0, \tag{17}$$

where σ is the hydrostatic stress, σ_{eq} is the equivalent stress defined by $\sigma_{eq} = \sqrt{(3/2)s_{ij}s_{ij}}$, s_{ij} are the deviator portions of stress components, α and σ_0 are material constants. The condition of coaxiality of the stress and strain-rate tensors can be written in the form

$$\xi_{ij} = \lambda s_{ij}, \tag{18}$$

where $\lambda > 0$ is the factor of proportionality. Thus the system of equations to be solved consists of the incompressibility equation and Eqs. (5), (17) and (18). It is of course necessary to take into account the condition of axial symmetry.

Using Eqs. (1) and (18) it is possible to find that

$$s_{rr} = -2s_{\theta\theta} = -2s_{\phi\phi}. \tag{19}$$

Substituting Eq. (19) into (17) gives

$$\alpha\sigma + \sqrt{3}\left(3s_{\theta\theta}^2 + s_{r\theta}^2\right)^{12} = \sigma_0. \tag{20}$$

It is convenient to introduce κ and γ by

$$s_{\theta\theta} = \kappa\cos\gamma/3 \quad \text{and} \quad s_{r\theta} = \kappa\sin\gamma/\sqrt{3}, \quad \kappa > 0. \tag{21}$$

Then, Eq. (20) transforms to

$$\alpha\sigma + \kappa = \sigma_0. \tag{22}$$

As before, assume that γ is independent of ρ. Then, substituting Eqs. (21) and (22) into (5) shows that the latter equations have a solution if and only if

$$\ln\left(1 - \alpha\frac{\sigma}{\sigma_0}\right) = A\ln\rho + P(\theta), \tag{23}$$

where A is an arbitrary constant and $P(\theta)$ is an arbitrary function of θ. Moreover, Eqs. (5) reduce to

$$\sqrt{3}\alpha(\alpha - 3\cos\gamma)\frac{d\gamma}{d\theta} = \Phi(\gamma, \theta), \tag{24}$$

where

$$\Phi(\gamma,\theta) = \alpha^2(A+3)\left(2+\sin^2\gamma\right) - 3\alpha A\cos\gamma - \sqrt{3}\cos\gamma\sin\gamma\cot\theta - 9A + 3\sqrt{3}\alpha\left(\sin\gamma\cot\theta - 2\sqrt{3}\cos\gamma\right) \tag{25}$$

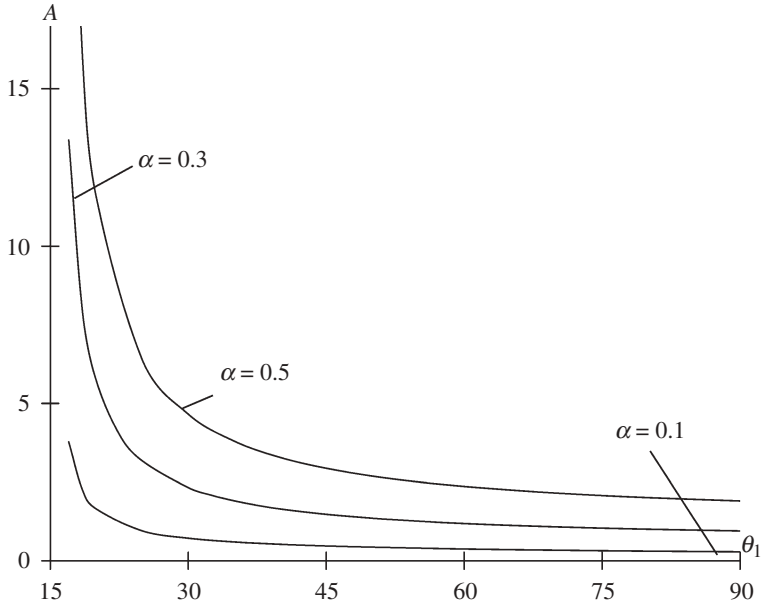

Fig. 8. Variation of A-value with the angle θ_1 at different values of α and $\theta_0 = 15^\circ$

and

$$\sqrt{3}(\alpha - 3\cos\gamma)\frac{dP}{d\theta} = \sin\gamma\Big[A(3 - \alpha\cos\gamma) - \sqrt{3}\alpha\Big(\sin\gamma\cot\theta + \sqrt{3}\cos\gamma\Big)\Big]. \tag{26}$$

It follows from Eq. (18) that

$$\frac{\xi_{\theta\theta}}{\xi_{r\theta}} = \frac{s_{\theta\theta}}{s_{r\theta}}. \tag{27}$$

Substituting Eq. (1) and (21) into (27) gives

$$\frac{dh}{d\theta} = 2\sqrt{3}h\tan\gamma. \tag{28}$$

Equations (24), (26) and (28) should be solved numerically to find the distribution of stress and velocity.

The condition $u_\rho < 0$ implies that $\xi_{\theta\theta} < 0$ and, then, Eq. (18) that $s_{\theta\theta} < 0$. The latter condition and (21) result in $\cos\gamma < 0$. Therefore, the angle γ should be within the interval $\pi/2 \le \gamma \le 3\pi/2$ and the maximum friction law requires that

$$\gamma = \frac{\pi}{2} \tag{29}$$

at $\theta = \theta_1$ and

$$\gamma = \frac{3\pi}{2} \tag{30}$$

at $\theta = \theta_0$. Then, it follows from (28) that the velocity field is singular near the friction surface. In particular, in the vicinity of the surface $\theta = \theta_0$ Eq. (28) can be rewritten in the form

$$\frac{dh}{d\theta} = \frac{2\sqrt{3}h}{(3\pi/2 - \gamma)} + o\left(\frac{1}{3\pi/2 - \gamma}\right) \tag{31}$$

and Eq. (24) in the form

$$\sqrt{3}\alpha^2\frac{d\gamma}{d\theta} = \Phi\left(\frac{3\pi}{2}, \theta_0\right) \equiv \Phi_0. \tag{32}$$

Combining Eqs. (31) and (32) it is possible to find that

$$h = H_0(\theta - \theta_0)^{-B_0} + o\left[(\theta - \theta_0)^{-B_0}\right] \quad \text{as } \theta \to \theta_{\mathrm{o}},\ B_0 = 6\alpha^2/\Phi_0, \tag{33}$$

Since the condition $h \to \infty$ has no physical sense, B_0 must satisfy the condition $B_0 < 0$. The latter condition will be checked *a posteriori*. If $B_0 < 0$ Eq. (33) shows that $h = 0$ at the friction surface and thus sticking occurs. Nevertheless, the equivalent strain rate can approach infinity at the surface if $m_0 = -1 - B_0 < 0$. Using similar arguments it is possible to show that

$$h = H_1(\theta_1 - \theta)^{-B_1} + o\left[(\theta_1 - \theta)^{-B_1}\right], \quad B_1 = 6\alpha^2/\Phi_1, \quad \Phi_1 = \Phi\left(\frac{\pi}{2}, \theta_1\right) \tag{34}$$

in the vicinity of the friction surface $\theta = \theta_1$. As before, a necessary condition for the existence of the solution is $B_1 < 0$ and the equivalent strain rate approaches infinity at $\theta = \theta_1$ if $m_1 = -1 - B_1 < 0$. The numerical solution to Eq. (28) in the interval $\pi/2 + \delta \le \theta \le 3\pi/2 - \delta$, where $\delta \ll 1$, should be matched with the asymptotic expansions (33) and (34).

Equation (24) has been solved with the boundary conditions (29) and (30). This solution determines the value of A and, with the use of (25), the values of Φ_0 and Φ_1. The variation of A with θ_1 at different values of α and $\theta_0 = 15^\circ$ is illustrated in Fig. 8. As before, there is no natural boundary condition for Eq. (26). Therefore, to illustrate the dependence of stress components of the angle θ, Eq. (26) has been solved with the condition $P = 0$ at $\theta = \theta_0$ and, then, Eqs. (21)–(23) have been used. The variation of dimensionless stress components with θ is shown in Figs. 9 through 11 at $\rho = 1$. The parameters of the process and material used are shown in the Figures. The solution to Eq. (28) satisfying the condition (15) is shown in Fig. 12 for different values of α.

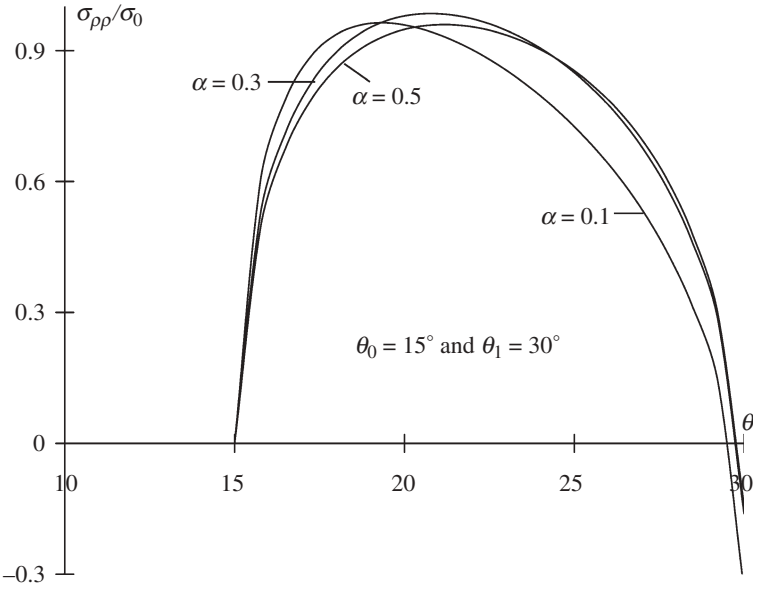

Fig. 9. Variation of the dimensionless stress $\sigma_{\rho\rho}/\sigma_0$ with the angle θ at $\rho = 1$

5 Analysis of the solutions

Consider the solution based on the double-shearing model. It is of interest to study the solution behavior in the vicinity of the frictional surfaces. It is known that the velocity field is singular near the maximum friction surfaces [15], [17]. Moreover, its asymptotic behavior is the same as in rigid perfectly/plastic solutions [16]. Using this property of the velocity field, the strain rate intensity factor has been introduced in [16] in the theory of rigid perfectly plastic solids. The concept of the strain rate intensity factor has been extended to material obeying Spenser's model in [17]. This concept can be used to describe the material behavior in the vicinity of surfaces with high friction [18], [19]. A distinguished feature of the problem under consideration is that there are two maximum friction surfaces. Therefore, it is possible to compare the two strain rate intensity factors and, based on this comparison, to make a conclusion on the intensity of physical processes in narrow layers near the frictional interfaces.

Using Eqs. (1) and (12) the shear strain rate is expressed as

$$\xi_{\rho\theta} = \frac{3Qh \sin 2\psi}{2\rho^3(\sin\phi + \cos 2\psi)}. \tag{35}$$

Obviously, $|\xi_{\rho\theta}| \to \infty$ as $\theta \to \theta_0$ and $\theta \to \theta_1$. By definition [16], the strain rate intensity factor is the coefficient of the main singular term in the expansion

$$\xi_{eq} = \sqrt{\frac{2}{3}\xi_{ij}\xi_{ij}} = \frac{D}{\sqrt{s}} + o\left(\frac{1}{\sqrt{s}}\right) \quad \text{as } s \to 0, \tag{36}$$

where ξ_{eq} is the equivalent strain rate, D is the strain rate intensity factor and s is the distance from the friction surface. Equation (7) in the vicinity of the friction surface $\theta = \theta_0$ can be represented in the form

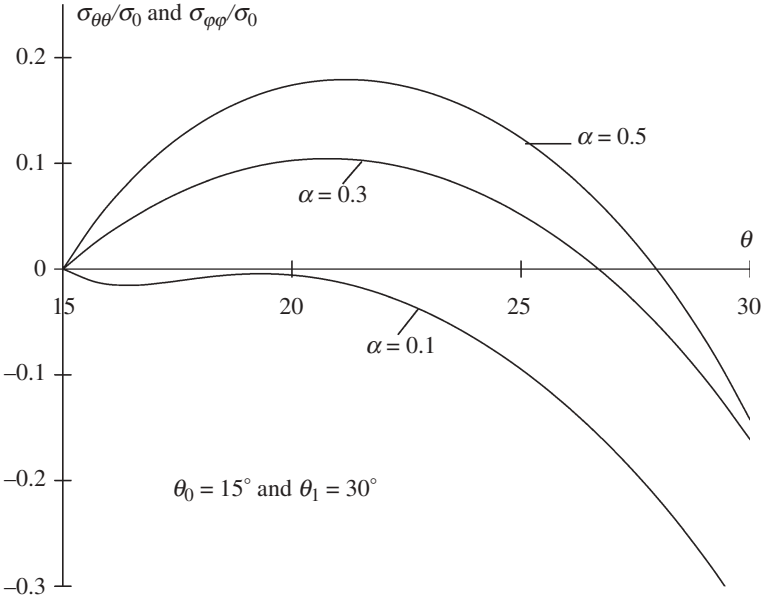

Fig. 10. Variation of the dimensionless stresses $\sigma_{\theta\theta}/\sigma_0$ and $\sigma_{\varphi\varphi}/\sigma_0$ with the angle θ at $\rho = 1$

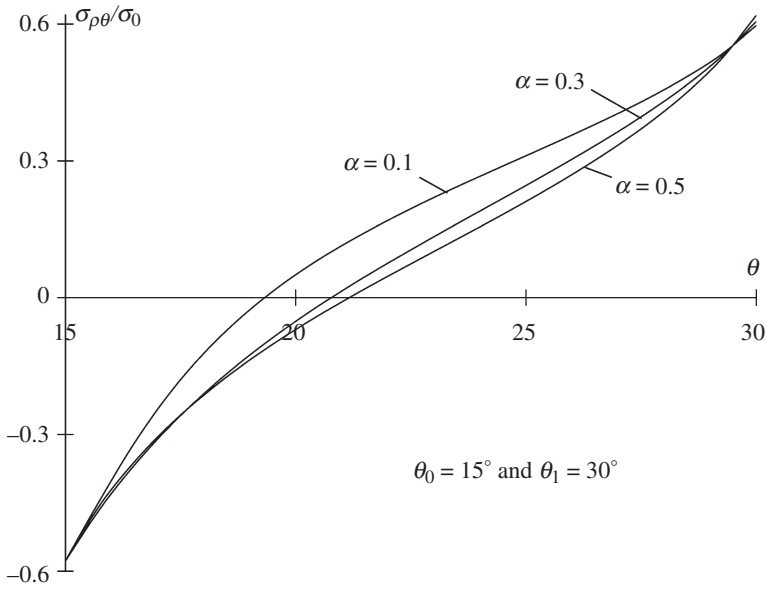

Fig. 11. Variation of the dimensionless stress $\sigma_{\rho\theta}/\sigma_0$ with the angle θ at $\rho = 1$

$$\frac{d\psi}{d\theta} = \frac{A_0}{\psi + \pi/4 + \phi/2} + o\left(\frac{1}{\psi + \pi/4 + \phi/2}\right), \tag{37}$$

where

$$A_0 = \frac{\cos\phi(n - \sin\phi) + \cot\theta_0 \sin\phi(1 + \sin\phi)}{4\sin\phi}. \tag{38}$$

Integrating Eq. (37) gives

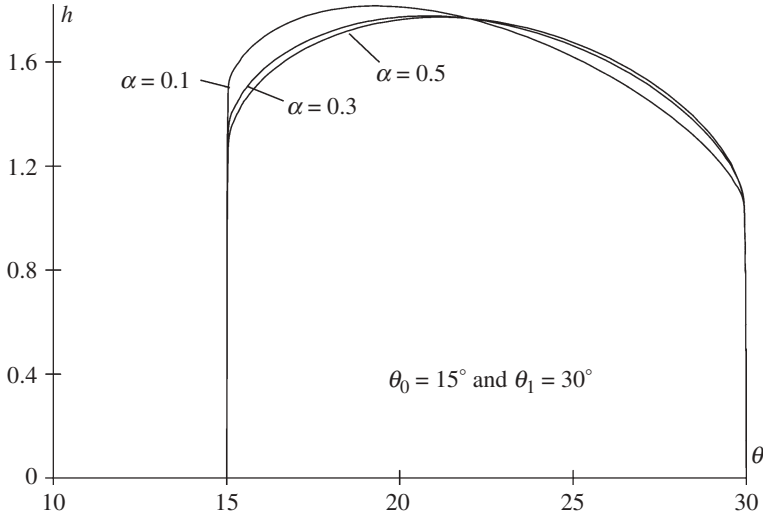

Fig. 12. Variation of h with the angle θ

$$\left(\psi+\frac{\pi}{4}+\frac{\phi}{2}\right)^2=2A_0(\theta-\theta_0) \tag{39}$$

to leading order. On the other hand, Eq. (35) can be expanded in the vicinity of the point $\psi=-(\pi/4+\phi/2)$ to give

$$\xi_{\rho\theta}=-\frac{3Qh_0}{4\rho^3(\psi+\pi/4+\phi/2)}+o\left(\frac{1}{\psi+\pi/4+\phi/2}\right), \tag{40}$$

where h_0 is the value of h at $\psi=-\pi/4-\phi/2$. Combining Eqs. (39) and (40) leads to

$$\xi_{\rho\theta}=-\frac{3Qh_0}{4\rho^3\sqrt{2A_0}\sqrt{\theta-\theta_0}} \tag{41}$$

to leading order. Since all strain rate components, except $\xi_{\rho\theta}$, are bounded at

$$\psi=-\pi/4-\phi/2,$$

$$\xi_{eq}=\frac{2}{\sqrt{3}}\left|\xi_{\rho\theta}\right| \tag{42}$$

as $\theta\to\theta_0$. Moreover, in the case under consideration s involved in (36) is $s=\rho(\theta-\theta_0)$. Therefore, combining Eqs. (36), (41) and (42) gives

$$D_0=\frac{\sqrt{3}Qh_0}{2\sqrt{2A_0}\rho^{5/2}}, \tag{43}$$

where D_0 is the value of D at the friction surface $\theta=\theta_0$. In the same manner it is possible to find that

$$D_1=\frac{\sqrt{3}Qh_1}{2\sqrt{-2A_1}\rho^{5/2}}, \tag{44}$$

where D_1 is the value of D at the friction surface $\theta=\theta_1$, h_1 is the value of h at $\psi=\pi/4+\phi/2$ and

$$A_1=\frac{\cos\phi(\sin\phi-n)+\cot\theta_1\sin\phi(1+\sin\phi)}{4\sin\phi}. \tag{45}$$

The variation of the strain rate intensity factors with ρ is obvious from (43) and (44). It is of interest to find the ratio $d=D_0/D_1$ at the same value of ρ. It follows from (43) and (44) that

$$d=\frac{h_0\sqrt{-A_1}}{h_1\sqrt{A_0}}. \tag{46}$$

The value of d has been calculated by means of the solution to Eqs. (15), (38) and (45). The dependence of d on process and material parameters is shown in Fig. 13. It is interesting to mention that the value of d can be either less or larger than 1. According to the concept of strain rate intensity factor [18], [19], this means that physical processes are more intensive in the vicinity of the friction surface $\theta=\theta_0$ at $\theta_1>\theta_*$ and in the vicinity of the friction surface $\theta=\theta_1$ at $\theta_1<\theta_*$. Here θ_* is the value of θ_1 at which $d=1$. Another possible interpretation of this result is that the thickness of the layer of intensive deformation is larger at the surface $\theta=\theta_0$ than at the surface $\theta=\theta_1$ if $\theta_1>\theta_*$ and vice versa.

Consider the solution based on the coaxial model. As in the case of the previous solution, it is of main interest to study the solution behavior in the vicinity of the friction surfaces. Figure 14 demonstrates the dependence of m_0 and m_1 on process and material parameters. In particular, it is seen from this figure that the inequalities $B_0<0$ and $B_1<0$ are satisfied. Therefore,

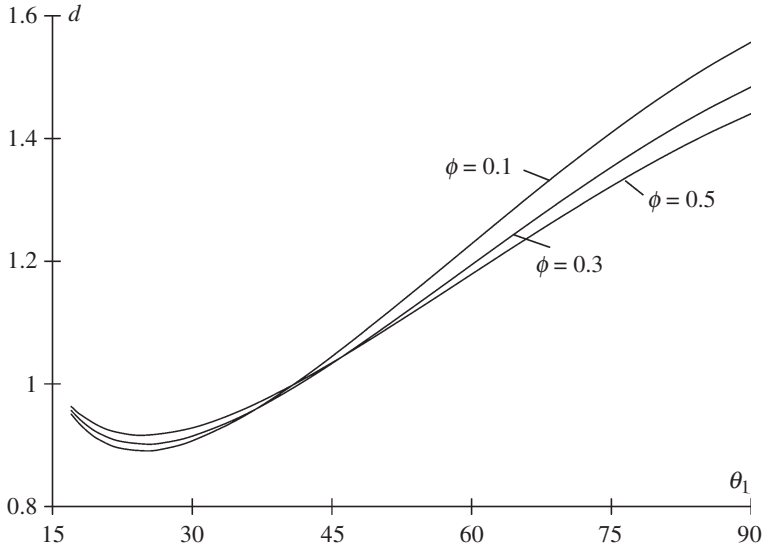

Fig. 13. Variation of the ratio of strain rate intensity factors with the angle θ_1 at different values of ϕ and $\theta_0 = 15^\circ$

sticking occurs at the friction surfaces, as follows from (33) and (34). It is one of essential differences of the solution based on the coaxial model from the solution based on the double-shearing model. In the latter case, sliding occurs at the friction surfaces (Fig. 7). In the vicinity of the friction surfaces the equivalent strain rate is proportional to $dh/d\theta$, since $|dh/d\theta| \to \infty$ and the other terms involved in the expression for the equivalent strain rate are bounded.

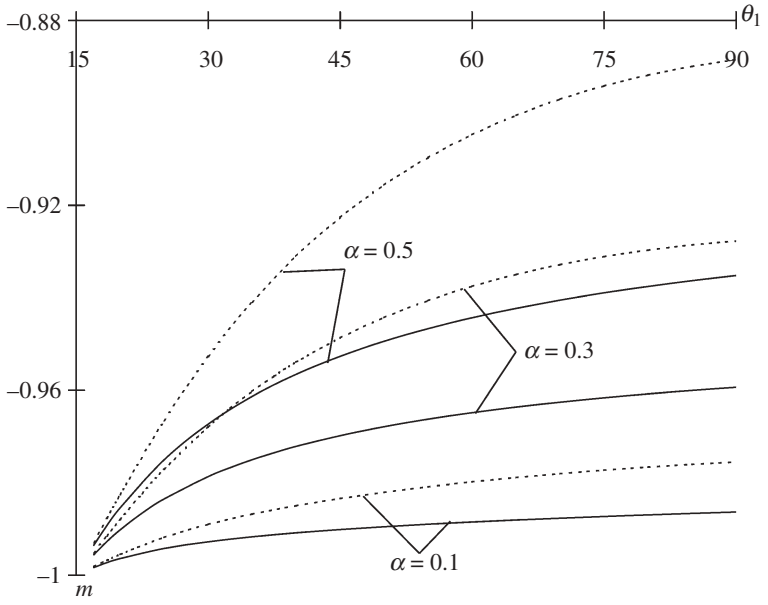

Fig. 14. Variation of m-value with the angle θ_1 at different values of α and $\theta_0 = 15^\circ$ (solid curves correspond to m_0 and dashed curves to m_1)

Figure 14 shows that the order of singularity in the solution based on the coaxial model is dependent on process and material parameters whereas in the case of the solution based on the double-shearing model the order of singularity is always equal to $-1/2$. It is the second essential difference between the two solutions. It is also seen from Fig. 14 that the order of singularity in the solution based on the coaxial model is much higher than that in the solution based on the double-shearing model, and that the order of singularity at $\theta = \theta_1$ is always higher than at $\theta = \theta_0$. A very high order of singularity in the solution based on the coaxial model results in extremely high velocity gradients in the vicinity of the friction surfaces (Fig. 12).

6 Conclusions

Using two models of pressure-dependent plasticity, the double-shearing model and the coaxial model, the solutions for the flow of material between two rough conical walls have been proposed. Special attention has been devoted to the solution behavior near the friction surfaces where the maximum friction law has been assumed. A comparative study has shown that the qualitative behavior of the solutions is quite different in the vicinity of the friction surfaces, though the models are supposed to describe the same class of materials. In particular, the solution based on the double-shearing model requires the sliding regime whereas the solution based on the coaxial model requires the sticking regime. Combining this result and experimental observations can constitute a basis for selecting the specific model of pressure-dependent plasticity for particular applications. Moreover, the former solution is singular such that the equivalent strain rate follows an inverse square root rule in the vicinity of the friction surfaces (see Eqs. (41) and (42)). The latter solution is also singular. However, the order of singularity depends on the process and material parameters (Fig. 14). Combining this result and the known asymptotic behavior of rigid perfectly/plastic solutions near the maximum friction surfaces [16] can constitute another basis for selecting the specific model of pressure-dependent plasticity. For instance, the solution based on the double-shearing model (but not the solution based on the coaxial model) and rigid perfectly/plastic solution show the same qualitative behavior in the vicinity of maximum friction surfaces. Since models of pressure-dependent plasticity are sometimes used to describe traditional metals (such metals are a typical area of applications of classical plasticity), for example [13], the double-shearing model has an advantage over the coaxial model.

The problem considered includes two surfaces of maximum friction. It is an advantage for verifying theories based on the concept of strain rate intensity factor, for example [18], [19], because it is possible to reveal a qualitative effect of the magnitude of the stress intensity factor on physical processes in a narrow material layer near the friction surface without determining parameters involved in the theories. In particular, Fig. 13 demonstrates that the physical processes are more intensive in the vicinity of the surface $\theta = \theta_0$ at larger θ_1 and in the vicinity of the surface $\theta = \theta_1$ if the value of θ_1 is close to the value of θ_0.

Results obtained can be useful in numerical simulation of more complicated problems. In particular, the qualitative behavior of solutions near the friction surface is solely controlled by the conditions at this surface. Therefore, it may be important for developing numerical codes that the maximum friction law leads to sticking when the coaxial model is adopted and to sliding when the double-shearing model is adopted. It may also be important that the solutions are singular near the maximum friction surfaces, and the order of singularity is determined by (36) and (41). It may require special numerical methods. Moreover, the velocity gradient is very

high at the friction surface (especially in the case of the coaxial model), which can lead to additional numerical difficulties.

The solutions can be adopted for approximate analysis of tube drawing [25].

Acknowledgement

This research was supported by INTAS through grant 04-83-2723 and the Russian Foundation for Basic Research through grant 05-01-00153.

References

[1] Sokolovskii, V. V.: Plane and axisymmetric equilibrium of plastic material between rigid walls. Prikl. Mat. Mekh. **14**, 75–92 (1950) [in Russian].
[2] Shield, R. T.: Plastic flow in a converging conical channel. J. Mech. Phys. Solids **3**, 246–258 (1955).
[3] Alexandrov, S., Barlat, F.: Axisymmetric plastic flow of an F.C.C. lattice metal in an infinite converging channel. Mech. Solids **32**, 125–131 (1997). [Trans. from Russian].
[4] Alexandrov, S., Barlat, F.: Modeling axisymmetric flow through a converging channel with arbitrary yield condition. Acta Mech. **133**, 57–68 (1999).
[5] Cristescu, N.: Plastic flow through conical converging dies, using a viscoplastic constitutive equation. Int. J. Mech. Sci. **17**, 425–433 (1975).
[6] Camenschi, G., Cristescu, N., Sandru, N.: High speed wire drawing. Arch. Mech. **31**, 741–755 (1979).
[7] Durban, D.: Axially symmetric radial flow of rigid/linear-hardening materials. ASME J. Appl. Mech. **46**, 322–328 (1979).
[8] Spencer, A. J. M.: Deformation of ideal granular materials. In: Mechanics of solids. The Rodney Hill 60th Anniversary Volume (Hopkins, H. G., Sewell, M. J., eds.), pp. 607–652. Oxford: Pergamon Press 1982.
[9] Ostrowska-Maciejewska, J., Harris, D.: Three-dimensional constitutive equations for rigid/perfectly plastic granular materials. Math. Proc. Camb. Phil. Soc. **108**, 153–169 (1990).
[10] Alexandrov, S.: Comparison of double-shearing and coaxial models of pressure-dependent plastic flow at frictional boundaries. Trans. ASME J. Appl. Mech. **70**, 212–219 (2003).
[11] Alexandrov, S., Lyamina, E.: Qualitative distinctions in the solutions based on the plasticity theories with Mohr-Coulomb yield criterion. J. Appl. Mech. Techn. Physics **46**, 883–890 (2005). [Trans. from Russian].
[12] Alexandrov, S., Harris, D.: Comparison of solution behavior for three models of pressure-dependent plasticity: a simple analytical example. Int. J. Mech. Sci. (accepted for publication).
[13] Spitzig, W. A., Sober, R. J., Richmond, O.: The effect of hydrostatic pressure on the deformation behavior of maraging and HY-80 steels and its implications for plasticity theory. Metallurg. Trans. **7A**, 1703–1710 (1976).
[14] Kao, A. S., Kuhn, H. A., Spitzig, W. A., Richmond, O.: Influence of superimposed hydrostatic pressure on bending fracture and formability of a low carbon steel containing globular sulfides. Trans. ASME J. Engng Mater. Technol. **112**, 26–30. (1990).
[15] Alexandrov, S.: Singular solutions in an axisymmetric flow of a medium obeying the double shear model. J. Appl. Mech. Techn. Physics **46**, 766–771 (2005). [Trans. from Russian].
[16] Alexandrov, S., Richmond, O.: Singular plastic flow fields near surfaces of maximum friction stress. Int J. Non-Linear Mech. **36**, 1–11 (2001).
[17] Alexandrov, S., Lyamina, E.: Singular solutions for plane plastic flow of pressure-dependent materials. Doklady Physics **47**, 308–311 (2002). [Trans. from Russian].
[18] Alexandrov, S.: Interrelation between constitutive laws and fracture criteria in the vicinity of friction surfaces. In: Physical Aspects of Fracture (Bouchaud, E., Jeulin, D., Prioul, C., Roux, S., eds.), pp. 179–190. Kluwer: Dordrecht 2001.

[19] Alexandrov, S., Goldshtein, R. V., Lyamina, E. A.: Developing the concept of the strain rate intensity factor in plasticity theory. Doklady Physics **48**, 131–133 (2003). [Trans. from Russian].
[20] Pemberton, C. S.: Flow of imponderable granular materials in wedge-shaped channels. J. Mech. Phys. Solids **13**, 351–360 (1965).
[21] Marshall, E. A.: The compression of a slab of ideal soil between rough plates. Acta Mech. **3**, 82–92 (1967).
[22] Alexandrov, S., Lyamina, E.: Plane-strain compression of material obeying the double-shearing model between rotating plates. Int. J. Mech. Sci. **45**, 1505–1517 (2003).
[23] Alexandrov, S., Lyamina, E.: Indentation of a wedge into a plastic medium governed by the double-shearing model. Mech. Solids **39**, 84–90 (2004). [Trans. from Russian].
[24] Alexandrov, S.: Steady penetration of a rigid cone into pressure-depedent plastic material. Int. J. Solids Struct. **43**, 193–205 (2006).
[25] Durban, D.: Drawing of tubes. Trans. ASME J. Appl. Mech. **47**, 736–740 (1980).

Authors' address: S. Alexandrov and E. Lyamina, Institute for Problems in Mechanics, Russian Academy of Sciences, 101-1 Prospect Vernadskogo, 119526 Moscow, Russia (E-mail: sergei_alexandrov@yahoo.com)